

Heterodimetallic Alkaline Earth Metal Amides: Synthesis, Structure, and Solvent-Induced Charge Separation of Homoleptic Calcium–Magnesium Hexamethyldisilazide

Lauren T. Wendell,[†] John Bender,[‡] Xuyang He,[†] Bruce C. Noll,[†] and Kenneth W. Henderson^{*,†}

Department of Chemistry and Biochemistry, University of Notre Dame, Notre Dame, Indiana 46556-5670, and Department of Chemistry, Grand Valley State University, Allendale, Michigan 49401-9403.

Received June 14, 2006

The heterodimetallic compound [(Me₃Si)₂NMg{μ-N(SiMe₃)₂}₂CaN(SiMe₃)₂], **3**, can be prepared as single-component crystals through manipulation of the equilibrium established on mixing the homometallic derivatives Mg[N(SiMe₃)₂]₂, **1**, and Ca[N(SiMe₃)₂]₂, **2**, in toluene/hexane solution. Specifically, doping solutions with a 30% molar excess of **1** is required in order to avoid cocrystallization with **2**. Complex **3** has been characterized by single-crystal X-ray diffraction and multinuclear NMR spectroscopy and is found to adopt a heterodimetallic Mg(μ₂-N)₂Ca ring structure in the solid state and in arene solutions. DFT computational studies confirm the experimentally observed variations in the metrical parameters between the homo- and heterodimetallic complexes. The calculations also indicate that the reaction to form **3** is close to being thermoneutral. Addition of pyridine to **3** results in asymmetric cleavage of the mixed-metal ring structure, in turn forming a kinetically stable, charge-separated “ate” species of the type [(Me₃Si)₂NCa·(pyr)_n]⁺[Mg{N(SiMe₃)₂}₃]⁻, **4**. The three bases **1**, **2**, and **4** react with propiophenone in pyridine media at ambient temperature to give high *Z* stereoselectivities of ≥98%.

Introduction

Alkali and alkaline earth metal amides are two of the most widely used classes of polar organometallic reagents.^{1,2} Their applications include serving as versatile reagents in organic synthesis,^{3–5} as metathesis reagents in the preparation of inorganic compounds,⁶ and also as catalysts in polymerization reactions.⁷ This has led to a great deal of attention being directed toward elucidating their structures both in solution⁸ and in the solid state.^{9–11} Hexamethyldisilazide (HMDS) is one of the most studied amide ligands for synthetic applications as well as for

structural investigations.¹² LiHMDS, NaHMDS, and KHMDS are all commercially available, and approaching one hundred crystal structures containing these bases have appeared.¹³ Similarly, the alkaline earth metal bisexamethyldisilazides have played a central role in developing the synthetic and structural

* Corresponding author. E-mail: khenders@nd.edu. Fax: +1 574 631 6652. Tel: +1 574 631 8025.

[†] University of Notre Dame.

[‡] Grand Valley State University.

(1) (a) Beswick, M. A.; Wright, D. S. In *Comprehensive Organometallic Chemistry II*; Abel, E. W., Stone, F. G. A., Wilkinson, G., Eds.; Pergamon: Oxford, 1995; Vol. 1, p 1. (b) *The Chemistry of Organolithium Compounds*; Rappoport, Z., Marek, I., Eds.; Wiley: New York, 2004. (c) Majewski, M.; Gleave, D. M. *J. Organomet. Chem.* **1994**, *470*, 1. (d) Wakefield B. J. *Organolithium Methods*; Academic Press: London, 1988. (e) Schlosser, M. In *Organometallics in Synthesis*, 2nd Edition; Schlosser, M. Ed.; Wiley: New York, 2002; p 1.

(2) (a) Henderson, K. W.; Kerr, W. J. *Chem. Eur. J.* **2001**, *7*, 3430. (b) Wakefield B. J. *Organomagnesium Methods in Organic Synthesis*; Academic Press: London, 1995. (c) Lindsell W. E. In *Comprehensive Organometallic Chemistry*; Wilkinson, G., Stone, F. G. A., Abel, E. W., Eds.; Pergamon: Oxford, 1982; Vol. 1, p 155. (d) *Grignard Reagents: New Developments*; Richey, H. G., Ed.; Wiley: New York, 2000. (e) Alexander, J. S.; Ruhlandt-Senge, K. *Eur. J. Inorg. Chem.* **2002**, 2761. (f) Westerhausen, M. *Angew. Chem., Int. Ed.* **2001**, *40*, 2975.

(3) (a) Berrisford, D. J. *Angew. Chem., Int. Ed. Engl.* **1995**, *34*, 178. (b) Clayden J. *Organolithiums: Selectivity for Synthesis*; Pergamon: Oxford, 2002. (c) O'Brien P. J. *Chem. Soc., Perkin Trans. 1* **2001**, 95. (d) Heathcock, C. H. In *Comprehensive Organic Synthesis*; Trost, B. M., Fleming, I., Eds.; Pergamon: Oxford, 1991; Vol. 2, p 181. (e) Caine, D. In *Comprehensive Organic Synthesis*; Trost, B. M., Fleming, I., Eds.; Pergamon: Oxford, 1991; Vol. 3, p 1. (f) d'Angelo, J. *Tetrahedron* **1976**, *32*, 2979. (g) *Asymmetric Synthesis*; Morrison, J. D., Ed.; Academic Press: New York, 1983; Vols. 2 and 3. (h) Snieckus, V. *Chem. Rev.* **1990**, *90*, 879.

(4) (a) Crimmin, M. R.; Casely, I. J.; Hill, M. S. *J. Am. Chem. Soc.* **2005**, *127*, 2042. (b) Avent, A. G.; Crimmin, M. R.; Hill, M. S.; Hitchcock, P. B. *J. Organomet. Chem.* **2006**, *691*, 1242. (c) Avent, A. G.; Crimmin, M. R.; Hill, M. S.; Hitchcock, P. B. *Dalton Trans.* **2005**, 278. (d) Avent, A. G.; Crimmin, M. R.; Hill, M. S.; Hitchcock, P. B. *Organometallics* **2005**, *24*, 1184. (e) Becker, G.; Niemeyer, M.; Mundt, O.; Schwarz, W.; Westerhausen, M.; Ossberger, M. W.; Mayer, P.; Nöth, H.; Zhong, Z.; Dijkstra, P. J.; Feijen, J. *Z. Anorg. Allg. Chem.* **2004**, *630*, 2605.

(5) (a) Henderson, K. W.; Kerr, W. J.; Moir, J. H. *Tetrahedron* **2002**, *58*, 4573. (b) Anderson, J. D.; Garcia, P. G.; Hayes, D.; Henderson, K. W.; Kerr, W. J.; Moir, J. H.; Fondecarr, K. P. *Tetrahedron Lett.* **2001**, *42*, 7111. (c) Henderson, K. W.; Kerr, W. J.; Moir, J. H. *Synlett* **2001**, 1253. (d) Henderson, K. W.; Kerr, W. J.; Moir, J. H. *Chem. Commun.* **2001**, 1722. (e) Henderson, K. W.; Kerr, W. J.; Moir, J. H. *Chem. Commun.* **2000**, 479. (f) Carswell, E. L.; Hayes, D.; Henderson, K. W.; Kerr, W. J.; Russell, C. J. *Synlett* **2003**, 1017. (g) Bassindale, M. J.; Crawford, J. J.; Henderson, K. W.; Kerr, W. J. *Tetrahedron Lett.* **2004**, *45*, 4175.

(6) Lappert, M. F.; Power, P. P.; Sanger, A. R.; Srivastava, R. C. *Metal and Metalloid Amides: Syntheses, Structures and Physical and Chemical Properties*; Ellis Horwood Limited: Chichester, England, 1980.

(7) (a) Chisholm, M. H.; Gallucci, J. C.; Phomphrai, K. *Chem. Commun.* **2003**, 48. (b) Chisholm, M. H.; Gallucci, J. C.; Phomphrai, K. *Inorg. Chem.* **2005**, *44*, 8004. (c) Dove, A. P.; Gibson, V. C.; Marshall, E. L.; White, A. J. P.; Williams, D. J. *Dalton Trans.* **2004**, 570. (d) Harder, S.; Feil, F. *Organometallics* **2002**, *21*, 2268. (e) Harder, S.; Feil, F. Knoll, K. *Angew. Chem., Int. Ed.* **2001**, *40*, 4261. (f) Couper, S. A.; Mulvey, R. E.; Sherrington, D. C. *Eur. Polym. J.* **1998**, *34*, 1877.

(8) (a) Collum, D. B. *Acc. Chem. Res.* **1993**, *26*, 227. (b) Collum, D. B. *Acc. Chem. Res.* **1992**, *25*, 448. (c) Hilmersson, G. *Chem. Eur. J.* **2000**, *6*, 3069. (d) Zune, C.; Dubois, P.; Grandjean, J.; Kriz, J.; Dybal, J.; Lochmann, L.; Janata, M.; Vlcek, P.; Jerome, R. *Macromolecules* **1999**, *32*, 5477.

(9) (a) Williard P. G. In *Comprehensive Organic Synthesis*; Trost B. M., Fleming I., Eds.; Pergamon Press: New York, 1991; Vol. 1, p 1. (b) Mulvey, R. E. *Chem. Soc. Rev.* **1998**, 339. (c) Downard, A.; Chivers, T. *Eur. J. Inorg. Chem.* **2001**, 2193. (d) Pauer, F.; Power, P. P. In *Lithium Chemistry: A Theoretical and Experimental Overview*; Sapse, A. M., Schleyer, P. v. R., Eds.; Wiley: New York, 1995; p 295.

organometallic chemistry of the group 2 elements.^{14,15} These compounds form an isostructural series of three-coordinate ring dimers in the solid state.^{16,17} In addition, several examples of heterodimetallic HMDS complexes composed of two different alkali metals (Li–Na, Li–K, and Na–K)¹⁸ and also an alkali metal in combination with an alkaline earth metal (Li–Mg,¹⁹ Li–Ca,²⁰ K–Mg,²¹ Rb–Mg,²¹ and K–Ca²²) have been reported. Such complexes can be considered as “ates”, with the more electronegative metals dominating the structural arrangement adopted. A somewhat surprising omission from this list is any example of a heterodimetallic complex containing a pair of alkaline earth metals. From a broader perspective, only a small number of compounds that contain two different group 2 metals have been crystallographically characterized, and these are mainly confined to carboxylic acid derivatives²³ or species where the metals are employed simply as solvated counterions.²⁴ In fact, the Sr/Ba phenoxide [H₂Sr₆Ba₂(μ₅-O)₂(OPh)₁₄(HMPA)₆], prepared by

(10) Markies, P. R.; Akkerman, O. S.; Bickelhaupt, F.; Smeets, W. J. J.; Spek, A. L. *Adv. Organomet. Chem.* **1991**, *32*, 147.

(11) (a) Henderson, K. W.; Williard, P. G. *Organometallics* **1999**, *18*, 5620. (b) Armstrong, D. R.; Henderson, K. W.; Kennedy, A. R.; Kerr, W. J.; Mair, F. S.; Moir, J. H.; Moran, P. H.; Snaith, R. *Dalton Trans.* **1999**, *22*, 4063. (c) Armstrong, D. R.; Carstairs, A.; Henderson, K. W. *Organometallics* **1999**, *18*, 3589. (d) Clegg, W.; Henderson, K. W.; Horsburgh, L.; Mackenzie, F.; Mulvey, R. E. *Chem. Eur. J.* **1998**, *4*, 53. (e) Clegg, W.; Craig, F. J.; Henderson, K. W.; Kennedy, A. R.; Mulvey, R. E.; O’Neil, P. A.; Reed, D. *Inorg. Chem.* **1997**, *36*, 6238. (f) Henderson, K. W.; Dorigo, A. E.; Liu, Q. Y.; Williard, P. G. *J. Am. Chem. Soc.* **1997**, *119*, 11855. (g) Henderson, K. W.; Dorigo, A. E.; Mulvey, R. E. *J. Organomet. Chem.* **1996**, *518*, 139. (h) Clegg, W.; Henderson, K. W.; Mulvey, R. E.; O’Neil, P. A. *J. Chem. Soc., Chem. Commun.* **1994**, 769. (i) Henderson, K. W.; Mulvey, R. E.; Clegg, W.; O’Neil, P. A. *Polyhedron* **1993**, *12*, 2535. (j) Clegg, W.; Henderson, K. W.; Mulvey, R. E.; O’Neil, P. A. *J. Chem. Soc., Chem. Commun.* **1993**, 969. (k) Clegg, W.; Henderson, K. W.; Mulvey, R. E.; O’Neil, P. A. *J. Organomet. Chem.* **1992**, *439*, 237.

(12) Lucht, B. L.; Collum, D. B. *Acc. Chem. Res.* **1999**, *32*, 1035, and references therein.

(13) Allen, F. H. *Acta Crystallogr.* **2002**, *B58*, 380.

(14) (a) Wannagat, U.; Kuckertz, H. *Angew. Chem.* **1963**, *75*, 95. (b) Wannagat, U.; Autzen, H.; Wismar, H.-J. *Z. Anorg. Allg. Chem.* **1972**, *394*, 254. (c) Bürger, H.; Forker, C.; Goubeau, J. *Montash. Chem.* **1965**, *96*, 597. (d) Nöth, H.; Schlosser, D. *Inorg. Chem.* **1983**, *22*, 2700.

(15) (a) Westerhausen, M. *Coord. Chem. Rev.* **1998**, *176*, 157. (b) Westerhausen, M. *Inorg. Chem.* **1991**, *30*, 96.

(16) (a) Westerhausen, M.; Schwarz, W. *Z. Anorg. Allg. Chem.* **1992**, *609*, 39. (b) Westerhausen, M.; Schwarz, W. *Z. Anorg. Allg. Chem.* **1991**, *604*, 127. (c) Westerhausen, M.; Schwarz, W. *Z. Anorg. Allg. Chem.* **1991**, *606*, 177.

(17) Vaartstra, B. A.; Huffman, J. C.; Streib, W. E.; Caulton, K. G. *Inorg. Chem.* **1991**, *30*, 121.

(18) Williard, P. G.; Nichols, M. A. *J. Am. Chem. Soc.* **1991**, *113*, 9671.

(19) (a) Kennedy, A. R.; Mulvey, R. E.; Rowlings, R. B. *J. Am. Chem. Soc.* **1998**, *120*, 7816. (b) Forbes, G. C.; Kennedy, A. R.; Mulvey, R. E.; Rodger, P. J. A.; Rowlings, R. B. *J. Chem. Soc., Dalton Trans.* **2001**, 1477. (c) Forbes, G. C.; Kennedy, A. R.; Mulvey, R. E.; Rodger, P. J. A. *Chem. Commun.* **2001**, 1400.

(20) (a) Davies, R. P. *Inorg. Chem. Commun.* **2000**, *3*, 13. (b) Kennedy, A. R.; Mulvey, R. E.; Rowlings, R. B. *J. Organomet. Chem.* **2002**, *648*, 288.

(21) Forbes, G. C.; Kennedy, A. R.; Mulvey, R. E.; Roberts, B. A.; Rowlings, R. B. *Organometallics* **2002**, *21*, 5115.

(22) He, X.; Noll, B. C.; Beatty, A.; Mulvey, R. E.; Henderson, K. W. *J. Am. Chem. Soc.* **2004**, *126*, 7444.

(23) (a) Schauer, C. K.; Anderson, O. P. *Inorg. Chem.* **1988**, *27*, 3118. (b) Stadnicka, K.; Glazer, A. M. *Acta Crystallogr., Sect. B* **1980**, *36*, 2977. (c) Matsui, M.; Watanabe, T.; Kamijo, N.; Lapp, R. L.; Jacobson, R. A. *Acta Crystallogr., Sect. B* **1980**, *36*, 1081. (d) Maruyama, H.; Tomiie, Y.; Mizutani, I.; Yamazaki, Y.; Uesu, Y.; Yamada, N.; Kobayashi, J. *J. Phys. Soc. Jpn.* **1967**, *23*, 899. (e) Stadnicka, K.; Glazer, A. M. *Acta Crystallogr., Sect. B* **1984**, *40*, 139. (f) Hofstatter, G.; Prandl, W.; Bruckel, T.; Hiller, W. *Acta Crystallogr., Sect. B* **1994**, *50*, 448. (g) Arriortua, M. I.; Insausti, M.; Urtiaga, M. K.; Via, J.; Rojo, T. *Acta Crystallogr., Sect. C* **1992**, *48*, 779. (h) Kiosse, G. A.; Razdobreev, I. M.; Malinovskii, T. I. *Dokl. Akad. Nauk* **1985**, *282*, 318.

(24) (a) Behr, J. P.; Lehn, J. M.; Moras, D.; Thierry, J. C. *J. Am. Chem. Soc.* **1981**, *103*, 701.

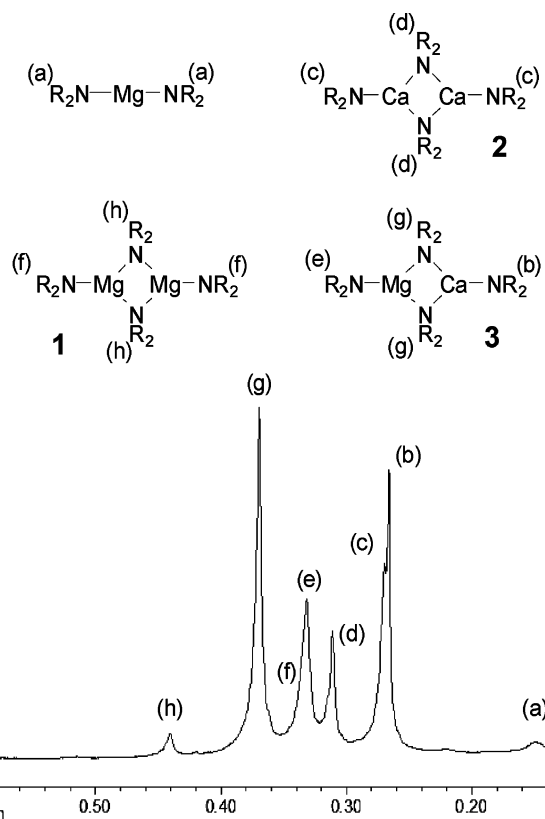


Figure 1. ¹H NMR spectrum of an equilibrium mixture containing **1**, **2**, and **3** in toluene-*d*₈ at 25 °C (R = TMS).

Caulton and Chisholm, is the single reported example of a structurally characterized molecular cage complex containing two different types of alkaline earth metals.²⁵ We initiated a study to complete the series of s-block complexes supported by HMDS ligands by preparing heterodimetallic complexes of the alkaline earth metals.²⁶ This apparently straightforward objective resulted in the discovery of several unanticipated features concerning the nature of these complexes. We now report the synthesis, structural characterization, and dynamic solution behavior of a Mg–Ca heterodimetallic hexamethyldisilazide compound.

Results and Discussion

Synthesis and NMR Spectroscopic Data. We opted to begin our investigations by targeting the synthesis of a mixed Mg–Ca complex since both Mg(HMDS)₂, **1**, and Ca(HMDS)₂, **2**, are readily prepared,¹⁵ and furthermore we have also recently shown that these homometallic compounds are useful reagents in the stereoselective enolization of ketonic substrates.^{27,28} The ¹H NMR spectra obtained on mixing **1** and **2** in toluene-*d*₈ proved to be a convenient method for studying the reaction. Previously, Westerhausen established that **2** retains its dimeric ring structure in arene solution, whereas **1** forms a monomer/dimer mixture.¹⁵ Figure 1 shows the spectrum that results from

(25) Caulton, K. G.; Chisholm, M. H.; Drake, S. R.; Foltling, K.; Huffman, J. C. *Inorg. Chem.* **1993**, *32*, 816.

(26) For a recent review on the chemistry of mixed alkali–alkaline earth metal amide bases see: Mulvey, R. E. *Organometallics* **2006**, *25*, 1060.

(27) He, X. Y.; Allan, J. F.; Noll, B. C.; Kennedy, A. R.; Henderson, K. W. *J. Am. Chem. Soc.* **2005**, *127*, 6920.

(28) For related uses of magnesium bisamides see: (a) Bonafoux, D.; Bordeau, M.; Biran, C.; Cazeau, P.; Dunogues, J. *J. Org. Chem.* **1996**, *61*, 5532. (b) Lessene, G.; Tripoli, R.; Cazeau, P.; Biran, C.; Bordeau, M. *Tetrahedron Lett.* **1999**, *40*, 4037.

Table 1. NMR Data for Dimeric 1–3 in Toluene-*d*₈ at 295 K, Where t = Terminal and b = Bridging

		¹ H	¹³ C{ ¹ H}	²⁹ Si{ ¹ H}
1	Mg–N(SiMe ₃) _t	0.34	7.11	–35.95
	Mg–N(SiMe ₃) _b	0.44	8.10	–26.64
2	Ca–N(SiMe ₃) _t	0.27	6.46	–43.44
	Ca–N(SiMe ₃) _b	0.31	6.90	–36.69
3	Mg–N(SiMe ₃) _t	0.33	7.41	–32.00
	Ca–N(SiMe ₃) _t	0.27	6.28	–43.25
	Mg–Ca–N(SiMe ₃) _b	0.37	7.41	–32.00

mixing equimolar quantities of **1** and **2**, and it is apparent that several solution species are present.

Five of the signals are readily assigned to **1** and **2** by comparison with spectra of the authentic homometallic compounds (bridging and terminal for each dimer, as well as monomeric **1**). The size and chemical shift positions of the three remaining signals are consistent with the formation of a heterodimetallic dimer of the type [(Me₃Si)₂NMg{μ-N(SiMe₃)₂}₂-CaN(SiMe₃)₂], **3**. Specifically, the signals at δ 0.27 and 0.33 arise from the Ca–N(SiMe₃)_t and the Mg–N(SiMe₃)_t units, and the signal at δ 0.37 represents the two equivalent Mg–N(SiMe₃)_b–Ca units (where N(SiMe₃)_t and N(SiMe₃)_b are terminal and bridging HMDS groups). ¹³C and ²⁹Si NMR spectroscopic data also support the presence of a new heterodimetallic complex (Table 1). The chemical shift positions associated with the terminal group in **3** are very similar to those in the homometallic counterparts. However, the chemical shifts of the bridging groups of **3** lie between those of **1** and **2** for each nuclei. All of the solution data are therefore consistent with the formation of a mixed-metal heterodimeric complex, albeit as part of an equilibrium mixture with the homometallic analogues.

Variable-temperature ¹H NMR spectroscopic studies were carried out between 21 and –60 °C. The homometallic complexes **1** and **2** display two separate signals for the bridging and terminal HMDS throughout this temperature range. For the equilibrium mixture of **1**, **2**, and **3** the pattern is more complex due to overlapping of the signals within the small chemical shift range available (~δ 0.20). Nevertheless, at –60 °C the signals separate to show the presence of **1** (δ 0.42 and 0.40), **2** (δ 0.36 and 0.26), and **3** (0.43, 0.34, and 0.33). These data are consistent with retention of the dimeric structures at this temperature.

Next, crystallization of the heterodimetallic complex was attempted. Well-formed crystals were deposited from a 5:1 toluene/hexane solution containing equimolar quantities of **1** and **2** after cooling to –20 °C. Subsequent NMR spectroscopic and single-crystal X-ray analyses corroborated the synthesis of a new mixed-metal compound, but unfortunately it was accompanied by substantial contamination with **2**. More specifically, crystallography established that the ring heterodimer **3** was the major component present (85–90%), with the remaining content being the homometallic dimer **2**. This whole-molecule disorder manifests itself most notably as partial site disorder of the magnesium position by calcium. The presence of excess **2** within the individual crystals could also be observed by integration of their ¹H NMR spectra, where the signals at δ 0.27 and 0.31, corresponding to the Ca–N(SiMe₃)_t and the Ca–N(SiMe₃)_b groups of **2**, were 10–15% larger than expected for a 1:1 Mg/Ca mixture.

Cocrystallization was particularly problematic in this instance as it negated meaningful comparisons between the metrical parameters of homometallics **1** and **2** with heterodimetallic **3**. Efforts to overcome this issue by altering the solvent media or the crystallization temperature had little effect. Changing the

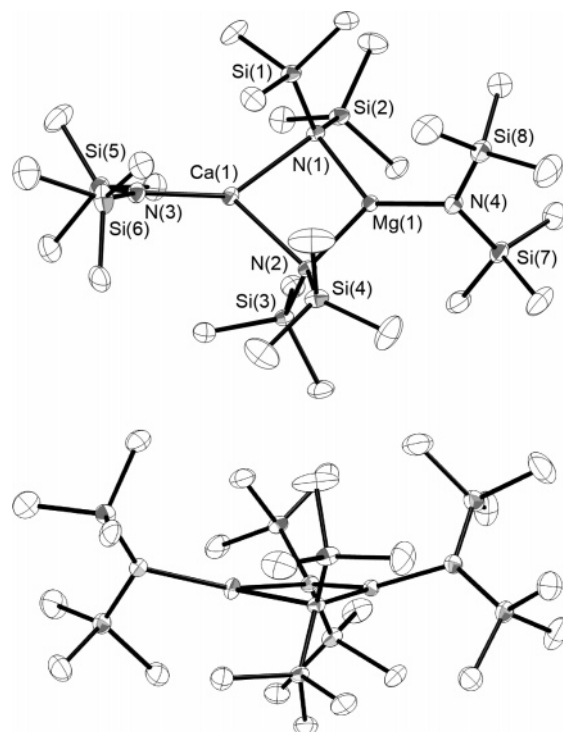


Figure 2. Molecular structure of **3** with hydrogen atoms removed (ellipsoids at 50% probabilities). Top: plane view of the central Mg(μ₂-N)₂Ca ring. Bottom: side view highlighting the *cisoid* orientation of the terminal HMDS groups.

concentration of the sample did affect the equilibrium position (as noted by NMR studies) due to the presence of the monomeric magnesium complex, but this strategy was not practical for crystallizations. We were intrigued by the observation that the crystals were consistently contaminated by **2** and never **1**. A possible explanation for this became apparent on close examination of the crystal structures of **1**–**3**.^{16a,b} Although all three compounds adopt three-coordinate dimeric ring structures, the geometries of **2** and **3** differ quite substantially from that of **1**. In particular, in **1** the two magnesium and four nitrogen centers of the dimer all lie in a single plane, whereas in **2** and **3** the central M₂N₂ rings are puckered, with the terminal HMDS groups orientated in a *cisoid* manner. We speculated that the similar size and overall gross shape adopted by **2** and **3** allowed their cocrystallization, whereas the planar structure of **1** excludes it from packing in an efficient manner with **3**. A series of doping experiments were carried out to determine if the equilibria between **1**, **2**, and **3** could be manipulated to reduce the quantity of calcium bisamide present in solution. NMR samples containing equimolar amounts of **1** and **2** were prepared as before, then spiked with various amounts of **1**. The resulting spectra indicated a shift in the equilibrium concentrations as desired, with depletion of **2** and an associated increase in **3**. Subsequently, the crystallization conditions were optimized such that crystals of pure **3** were prepared using 1.5:3.5 hexane/toluene mixtures containing a 30% molar excess of **1** over **2**.

Crystallographic Studies. X-ray analysis of the resulting crystals indicated no discernible cocrystallization with **2**. After modeling the disorder of one of the trimethylsilyl groups around Si(6) the largest peak in the final difference map is only 0.36 e[–]/Å³. This peak is located 0.973 Å from Si(7) and 0.906 Å from C(20). So, there are no significant peaks in the map, indicating no detectable contamination by **2**.

As shown in Figure 2, complex **1** contains a four-membered ring core with a pair of amide ligands bridging the metal centers

Table 2. Selected Bond Lengths (Å) and Angles (deg) for 1–3

1	2	3
Mg–N ^t 1.975(7)	Ca–N ^t 2.282(6)	Mg(1)–N(4) ^t 1.993(3)
Mg–N ^b 2.145(5)	Ca–N ^t 2.267(7)	Ca(1)–N(3) ^t 2.272(3)
Mg–N ^b 2.156(4)	Ca–N ^b 2.482(6)	Mg(1)–N(1) ^b 2.147(3)
N ^b –Mg–N ^b 95.5(2)	Ca–N ^b 2.520(6)	Mg(1)–N(2) ^b 2.136(3)
N ^b –Mg–N ^b 96.1(2)	Ca–N ^b 2.430(6)	Ca(1)–N(1) ^b 2.562(2)
N ^b –Mg–N ^t 131.9 ^a	Ca–N ^b 2.466(6)	Ca(1)–N(2) ^b 2.467(3)
N ^b –Mg–N ^t 132.2 [†]	N ^b –Ca–N ^b 88.0(2)	N(1) ^b –Mg(1)–N(2) ^b 101.24(10)
Mg–N ^b –Mg 84.2(2)	N ^b –Ca–N ^b 90.4(2)	N(1) ^b –Mg(1)–N(4) ^t 130.11(11)
Si–N ^b –Si 110.8(2)	N ^b –Ca–N ^t 132.9(2)	N(2) ^b –Mg(1)–N(4) ^t 127.21(11)
Si–N ^t –Si 117.3(4)	N ^b –Ca–N ^t 138.7(2)	N(1) ^b –Ca(1)–N(2) ^b 82.33(8)
Si–N ^t –Si 120.7(4)	N ^b –Ca–N ^t 134.4(2)	N(1) ^b –Ca(1)–N(3) ^t 143.04(9)
	N ^b –Ca–N ^t 133.4(2)	N(2) ^b –Ca(1)–N(3) ^t 132.97(9)
	Ca–N ^b –Ca 91.6(2)	Mg(1)–N(1) ^b –Ca(1) 86.35(8)
	Ca–N ^b –Ca 89.8(2)	Mg(1)–N(2) ^b –Ca(1) 89.05(9)
	Si–N ^b –Si 119.9(4)	Si(1)–N(1) ^b –Si(2) 113.77(14)
	Si–N ^b –Si 114.7(3)	Si(3)–N(2) ^b –Si(4) 114.46(14)
	Si–N ^t –Si 121.3(4)	Si(5)–N(3) ^t –Si(6) 122.81(15)
	Si–N ^t –Si 123.2(4)	Si(8)–N(4) ^t –Si(7) 119.87(15)

^a esd not available.

and with each metal binding additionally to a terminal amide group. This heterodimetallic structure with three-coordinate metal centers is consistent with our solution studies of this complex. The key bond lengths and angles within **3** are listed in Table 2 along with those of the homometallic complexes **1** and **2**. The Mg–N^b (where N^b = bridging amide) distances of 2.147(3) and 2.136(3) Å in **3** are very similar to those of 2.156(7) and 2.145(5) Å in **1**, with a mean contraction of only 0.009 Å. Similarly, the Ca–N^t (where N^t = terminal amide) bond distance of 2.272(3) Å in **3** lies between the two values of 2.282(6) and 2.267(7) Å in **2**. More significant changes are found for the Mg–N^t and the Ca–N^b bonds. The terminal Mg–N^t bond lengthens by 0.018 Å on moving from **1** (1.975(5) Å) to **3** (1.993(3) Å). Also, the mean Ca–N^b bonds (2.467(3) and 2.562(2) Å) in **3** lengthen by 0.040 Å compared with the homometallic derivative (2.430(6), 2.466(6), 2.482(6), and 2.520(6) Å).

The most notable changes in the angles of **3** compared with the homometallic precursors are associated with the two metal centers. Specifically, the N(1)–Mg(1)–N(2) angle widens by 5.4° and the N(1)–Ca(1)–N(2) angle narrows by 6.9°. Furthermore, the geometry around the magnesium in **3** is no longer planar, with the sum of the N–Mg–N angles being 358.6° and the metal sitting 0.142 Å out of the N(1)–N(2)–N(4) plane. In comparison, the sum of the N–Ca–N angles in **2** and **3** are similar at 358.3° and 358.9°, and the metal lies 0.164 Å out of the N(1)–N(2)–N(3) plane in **3**, which lies between the two values of 0.086 and 0.178 Å in **2**. Finally, the Mg(μ_2 -N)₂Ca ring is puckered with an angle of 11.2° between the N(1)–Mg(1)–N(2) and the N(1)–Ca(1)–N(2) planes, whereas this angle in **1** is 0.0° and in **2** is 5.2°.

Overall, the variations in bond lengths and angles in **3** compared to the homometallic precursors can be explained by considering the relative Lewis acidities of the metals. Magnesium is considerably smaller than calcium (ionic radii 0.86 Å, cf 1.26 Å),²⁹ resulting in a higher Lewis acidity. In turn, this leads to weakening of the Ca–N^b bonds, a widening of the internal ring angles at magnesium, and a concomitant narrowing of these angles at calcium. The Ca–N^t bonds are not strongly influenced by this change, but the increase in electron density at magnesium results in a slight lengthening of the Mg–N^t distance.

Table 3. Selected Bond Lengths (Å) and Angles (deg) for I–III at the B3LYP/6-311++G Level of Theory**

I	II	III
Mg–N ^t 2.010	Ca–N ^t 2.291	Mg–N ^t 2.023
Mg–N ^t 2.010	Ca–N ^t 2.299	Ca–N ^t 2.289
Mg–N ^b 2.184	Ca–N ^b 2.568	Mg–N ^b 2.172
Mg–N ^b 2.180	Ca–N ^b 2.515	Mg–N ^b 2.161
Mg–N ^b 2.180	Ca–N ^b 2.487	Ca–N ^b 2.593
Mg–N ^b 2.178	Ca–N ^b 2.473	Ca–N ^b 2.482
N ^b –Mg–N ^b 95.19	N ^b –Ca–N ^b 91.04	N ^b –Mg–N ^b 101.53
N ^b –Mg–N ^b 95.40	N ^b –Ca–N ^b 91.97	N ^b –Mg–N ^t 130.51
N ^b –Mg–N ^t 132.70	N ^b –Ca–N ^t 128.25	N ^b –Mg–N ^t 127.34
N ^b –Mg–N ^t 132.11	N ^b –Ca–N ^t 140.70	N ^b –Ca–N ^b 82.76
N ^b –Mg–N ^t 132.22	N ^b –Ca–N ^t 131.61	N ^b –Ca–N ^t 144.06
N ^b –Mg–N ^t 132.37	N ^b –Ca–N ^t 131.07	N ^b –Ca–N ^t 132.57
Mg–N ^b –Mg 84.63	Ca–N ^b –Ca 89.74	Mg–N ^b –Ca 88.98
Mg–N ^b –Mg 84.77	Ca–N ^b –Ca 87.03	Mg–N ^b –Ca 85.93
Si–N ^b –Si 111.24	Si–N ^b –Si 117.06	Si–N ^b –Si 114.64
Si–N ^b –Si 111.09	Si–N ^b –Si 115.27	SiN ^b –Si 113.68
Si–N ^t –Si 117.04	Si–N ^t –Si 122.90	Si–N ^t –Si 118.21
Si–N ^t –Si 118.48	Si–N ^t –Si 123.60	Si–N ^t –Si 122.06

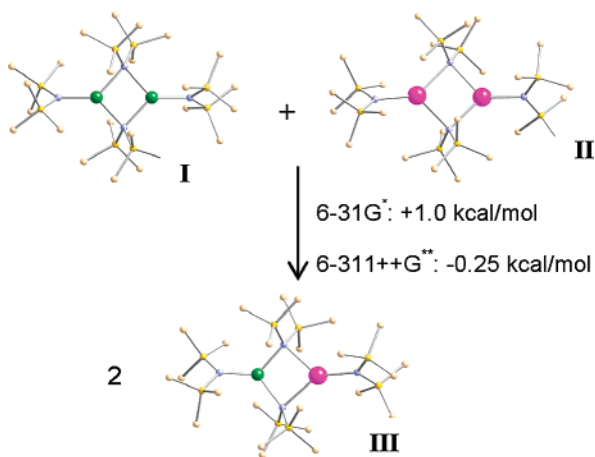
The possible role of stabilizing intramolecular agostic interactions between the methyl groups of HMDS and adjacent alkali and alkaline earth metal centers has been discussed in some detail.^{16,20b} In **3** only two relatively short Ca···CH₃ distances are present: Ca···C(1) at 2.890(5) Å involving a bridging HMDS unit and Ca···C(15) at 2.828(5) Å from the terminally bound HMDS group. This situation is similar to that in the unsymmetrical homometallic complex **2**, which has one of the calcium centers lying close to two methyl groups, 2.855 (bridging) and 2.833 Å (terminal), with the second calcium lying close to a single bridging methyl unit at 2.827 Å. All of the remaining Ca···CH₃ and Mg···CH₃ distances in **3** are >3.3 and >2.9 Å, respectively, and are unlikely to be of significance.

Computational Studies. A density functional theory (DFT) computational study was undertaken to further probe the structural analyses and also to investigate the energetics concerning the formation of **3**. The crystal structures of **1–3** were used as starting positions for geometry optimization at the B3LYP/6-31G* level of theory.³⁰ The geometries obtained were then reoptimized with the larger 6-311++G** basis set. A summary of the bond lengths and angles obtained for **I–III** is given in Table 3. Comparison of the calculated and

(29) Huheey, J. E.; Keiter, E. A.; Keiter, R. L. *Inorganic Chemistry: Principles of Structure and Reactivity*, 4th ed.; HarperCollins: New York, 1993.

(30) (a) Becke, A. D. *J. Chem. Phys.* **1993**, *98*, 5648. (b) Miehlich, B.; Savin, A.; Stoll, H.; Preuss, H. *Chem. Phys. Lett.* **1989**, *157*, 200. (c) Lee, C.; Yang, W.; Parr, R. G. *Phys. Rev. B.* **1988**, *37*, 785.

Scheme 1. Geometry-Optimized Structures of I–III



experimentally derived metrical parameters shows excellent agreement, with the individual bond lengths and angles in Tables 2 and 3 varying by less than 0.05 Å and 5° for the three compounds. The calculations therefore act as an independent verification that crystallographic data derived for **3** are valid. The absolute energies of **I–III** were used to estimate the relative stabilities of the homometallic and the heterodimetallic complexes. As shown in Scheme 1 the formation of two molecules of **III** from **I** and **II** is estimated to be favored by only -0.25 kcal/mol at the higher level of theory. This indicates that the reaction to form **3** from the homometallic complexes is close to being thermoneutral. Indeed, the calculations are consistent with the NMR solution studies, which indicate the coexistence of all three components in arene solution.

Reactions in Polar Solvents. Dissolution of **1** or **2** in polar solvents results in dissociation of the dimers to solvated monomers.¹⁵ The ^1H NMR spectra of **1** and **2** in pyridine- d_5 each display a single resonance centered at δ 0.34. We therefore expected that the ^1H NMR spectrum of **3** in pyridine- d_5 would similarly result in the appearance of a single peak in this region. As shown in Figure 3 a signal centered at δ 0.34 did indeed appear; however, two additional signals at δ 0.62 and δ 0.17 (3:1 ratio) were also present as the major components of the mixture. The large downfield chemical shift of the peak at δ 0.62 suggests trisamide anion formation, i.e. $[\text{M}\{\text{N}(\text{SiMe}_3)_2\}_3]^-$. We have previously prepared the $[\text{Ca}\{\text{N}(\text{SiMe}_3)_2\}_3]^-$ anion in pyridine- d_5 , and its ^1H NMR chemical shift position of δ 0.55 discounts its presence in this instance.²¹ The independent formation of the magnesium trisamide anion was therefore attempted by mixing equimolar quantities of KHMDS, $\text{Mg}(\text{HMDS})_2$, and 18-crown-6 in pyridine- d_5 to produce a charge-separated complex of the type $[\text{K}\cdot(18\text{-C-}6)\cdot(\text{pyr})_n]^+[\text{Mg}\{\text{N}(\text{SiMe}_3)_2\}_3]^-$. The resulting ^1H NMR spectrum displays a single peak at δ 0.62, supporting the formation of the magnesium trisamide anion. Furthermore, Mulvey has recently reported the characterization of $[\text{Mg}\{\text{N}(\text{SiMe}_3)_2\}_3]^-$ ions in the solid state.^{19c,31} The remaining upfield signal at δ 0.17 can therefore be assigned as a solvated calcium cation, $[\text{CaN}(\text{SiMe}_3)_2\cdot(\text{pyr})_n]^+$. The nuclearity and solvation of this cation are, as yet, unknown. Overall, in combination with the 3:1 ratio of the two signals, these data are consistent with formation of a charge-separated complex of the type $[\text{CaN}(\text{SiMe}_3)_2\cdot(\text{pyr})_n]^+[\text{Mg}\{\text{N}(\text{SiMe}_3)_2\}_3]^-$, **4**. Previously, Richey identified the formation of organomagnesiate ions by the addition of sequestering agents such as crowns and cryptands to diorganomagnesium compounds.^{32,33}

(31) Honeyman, G. W.; Kennedy, A. R.; Mulvey, R. E.; Sherrington, D. C. *Organometallics* **2004**, *23*, 1197.

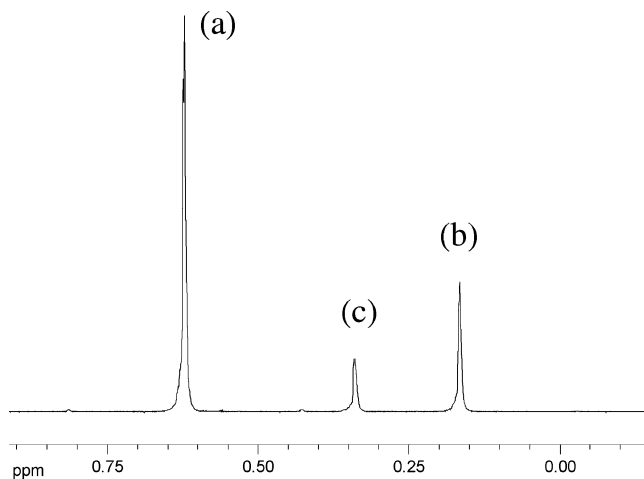


Figure 3. ^1H NMR spectrum on the dissolution of **3** in pyridine- d_5 at 25 °C: (a) $[\text{Mg}\{\text{N}(\text{SiMe}_3)_2\}_3]^-$, (b) $[\text{CaN}(\text{SiMe}_3)_2\cdot(\text{pyr})_n]^+$, and (c) solvated monomers $[\text{Mg}(\text{HMDS})_2\cdot(\text{pyr})_n]$ and $[\text{Ca}(\text{HMDS})_2\cdot(\text{pyr})_n]$.

^1H NMR spectroscopic studies proved useful in determining the mechanism by which **4** is formed. An EXSY experiment run at ambient temperature showed no exchange on the NMR time scale between **4** and the monometallic complexes. Nevertheless, complex **4** was slowly depleted over several days in pyridine- d_5 to afford solely the solvated monomers. Therefore, **4** is prepared as a kinetic product with the solvated monomers being thermodynamically preferred. Also, mixing individually prepared pyridine- d_5 solutions of **1** and **2** resulted in only a single signal at δ 0.34, indicating the presence of the solvated monomers. This is a revealing experiment, as it indicates that the heterodimetallic $\text{Mg}(\mu_2\text{-N})_2\text{Ca}$ ring in **3** is required in order to provide a pathway for charge separation to occur. Moreover, dissolution of crystalline **3** in toluene- d_8 followed by the addition of ≥ 4 molar equiv of pyridine- d_5 resulted in the appearance of **4**, in addition to the monomers. Under these conditions **4** equilibrated to the homometallic monomers within a few hours. In combination these data are consistent with the heterodimetallic molecule undergoing both symmetric and asymmetric cleavage in the presence of pyridine (Scheme 2). Asymmetric cleavage pathways to produce charge-separated complexes have significant precedence, most notably for boron hydrides but also for homoleptic magnesium aryloxides.^{34,35}

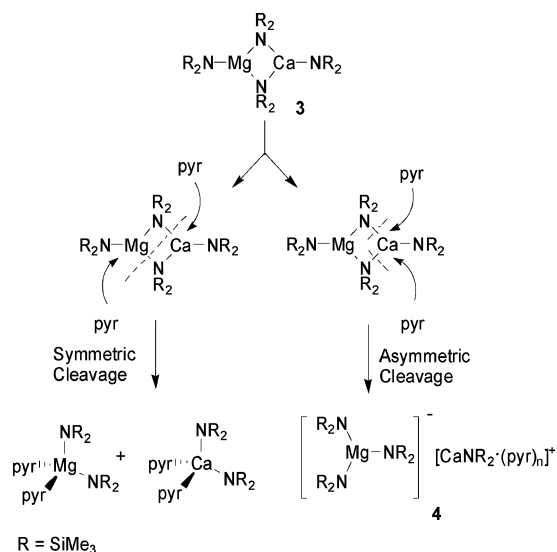
The enolization of propiophenone was used as a preliminary benchmark reaction to test the relative reactivity and stereoselectivity displayed by **4** in comparison to the homometallic compounds (Scheme 3).²¹ Separate (~ 0.1 M) pyridine- d_5 solutions of **1**, **2**, and **4** (generated in situ at $\sim 80\%$, with the remainder being monomers) were prepared and reacted with

(32) (a) Pajerski, A. D.; Kushlan, D. M.; Parvez, M.; Richey, H. G. *Organometallics* **2006**, *25*, 1206. (b) Pajerski, A. D.; Squiller, E. P.; Parvez, M.; Whittle, R. R.; Richey, H. G. *Organometallics* **2005**, *24*, 809. (c) Chubb, J. E.; Richey, H. G. *Organometallics* **2002**, *21*, 3661. (d) Hanawalt, E. M.; Richey, H. G. *J. Am. Chem. Soc.* **1990**, *112*, 4983. (e) Pajerski, A. D.; Parvez, M.; Richey, H. G. *J. Am. Chem. Soc.* **1988**, *110*, 2660. (f) Richey, H. G.; Kushlan, D. M. *J. Am. Chem. Soc.* **1987**, *109*, 2510. (g) Squiller, E. P.; Whittle, R. R.; Richey, H. G. *J. Am. Chem. Soc.* **1985**, *107*, 432. (h) Richey, H. G.; King, B. A. *J. Am. Chem. Soc.* **1982**, *104*, 4672.

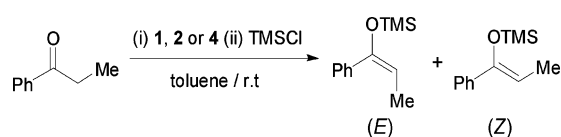
(33) For other examples of magnesia characterization see: (a) Viebrock, H.; Behrens, U.; Weiss, E. *Angew. Chem., Int. Ed. Engl.* **1994**, *33*, 1257. (b) Viebrock, H.; Abeln, D.; Weiss, E. *Z. Naturforsch. Teil B* **1994**, *49*, 89. (c) Harder, S.; Feil, F.; Repo, T. *Chem. Eur. J.* **2002**, *8*, 1991.

(34) *Boron Hydride Chemistry*; Muetterties, E. L., Ed.; Academic Press: New York, 1975.

(35) (a) Calabrese, J.; Cushing, M. A.; Ittel, S. D. *Inorg. Chem.* **1988**, *27*, 867. (b) Henderson, K. W.; Honeyman, G. W.; Kennedy, A. R.; Mulvey, R. E.; Parkinson, J. A.; Sherrington, D. C. *Dalton Trans.* **2003**, 1365.

Scheme 2. Solvation Pathways for **3**

Scheme 3



0.75 equiv of propiophenone at ambient temperature. Monitoring by ^1H NMR spectroscopy indicated that both **2** and **4** completely consumed the ketone within a few minutes, whereas the magnesium analogue required approximately 2 h for completion. These results are consistent with rate studies carried out by Richey, which found that organomagnesiates have similar or superior reactivity compared with the neutral reagent.³¹ Each reaction was then quenched using TMSCl, and the silyl enol ethers were analyzed by GC to determine the stereoselectivity of the bases. In all three instances the bases produced predominantly the *Z*-enolate with selectivities $\geq 98\%$. The preference for the *Z*-enolates is in accord with expectations for metal base-mediated enolization reactions conducted in polar solvents.³

Conclusions. Complex **3** is the first example of a heterodimetallic complex containing two alkaline earth metal amides to be structurally characterized. This is perhaps unsurprising considering the general similarities of the two metals under investigation, which leads to little, if any, preference for the formation of the mixed-metal complex. Indeed, this is reflected in the equilibrium mixture established on mixing the homometallic reagents **1** and **2** and also by the difficulty in preparing a pure sample of **3**. However, it is likely that the preparation of other combinations of alkaline earth metal heterodimetallics should be possible, especially for pairs of metals that are not direct periodic neighbors.

Although the discovery of the solvent-induced charge separation of **3** was unexpected, its solid-state structure provides some insight into why this reaction may occur. Comparison of heterodimetallic **3** with the homometallic calcium analogue **2** shows substantial weakening of the bonding to the bridging amide units due to the stronger interactions with the more Lewis acidic magnesium center. In turn, the bonding in compound **3** may be considered as already moving toward charge separation to form an "ate" species. Therefore, donor solvent attack takes place at the more sterically accessible calcium center, which leads to Ca–N bond cleavage and kinetic formation of the charge-separated complex **4**.

Finally, the observation of the differing reactivity of **4** compared with the homometallic complex **1** indicates that they react through distinct mechanisms. For the enolization reactions studied here this had no discernible effect on the resulting stereoselectivity of the bases. This is not surprising since the reactions were conducted in pyridine, which favors *Z*-selective enolizations.³ However, we expect that the involvement of charge-separated species will result in significant differences in the selectivities of these bases when appropriate conditions are applied.

Experimental Section

All operations were carried out using Schlenk techniques or inside an argon-filled glovebox.³⁶ All glassware was flame-dried under vacuum before use. Toluene and hexane were dried by passage through copper-based catalyst and molecular sieve columns (Innovative Technology). Propiophenone was purchased from Acros and distilled over CaH_2 under N_2 prior to use.³⁷ TMSCl was distilled under a N_2 atmosphere before use. $\text{Mg}(\text{HMDS})_2$ and $\text{Ca}(\text{HMDS})_2$ were prepared as described previously.^{22,38} Deuterated solvents were purchased from Cambridge Isotope Laboratories and were dried by storage over 4 Å molecular sieves. ^1H , ^{13}C , and ^{29}Si NMR spectra were recorded on Varian-300/500 or Bruker Avance-400 spectrometers at 25 °C. ^1H and ^{13}C NMR spectra were referenced internally to the residual signals of the deuterated solvents, and the ^{29}Si spectra were referenced to an external sample of TMSCl set at 0 ppm. IR spectra were recorded on a Nicolet Avatar 360 FTIR spectrophotometer through KBr plates as Nujol mulls. Melting points were recorded on a Meltemp apparatus. Mass spectrometry was run on a JEOL GCMate. GC experiments were performed on a Shimadzu GC-17A gas chromatograph fitted with a Rtx-5 fused Crossbond 5% diphenyl–95% dimethyl polysiloxane column (30 m, 0.25 mm i.d., 0.25 μm), using N_2 as carrier gas. Detection was by flame ionization, and the chromatograms were interpreted using GCsolution software. Elemental analyses were performed by Canadian Microanalysis Ltd.

Synthesis of $[\text{CaMg}\{\text{N}(\text{SiMe}_3)_2\}_4]$, **3.** In a drybox, 0.889 g of solid $\text{Mg}(\text{HMDS})_2$ (2.6 mmol) and 0.720 g of solid $\text{Ca}(\text{HMDS})_2$ (2.0 mmol) were added to a 50 mL Schlenk tube. The tube was removed from the drybox and charged with 7 mL of toluene. The solids were allowed to slowly solublize overnight while stirring. The solution was concentrated in vacuo to ~ 1.5 mL, and 3.5 mL of hexane was added. The cloudy solution was filtered through a glass sinter filled with Celite, and the filtrate was cooled to -20 °C. Clear, colorless crystals were deposited on standing overnight (0.25 g, 35%); mp 123 °C. ^1H , ^{13}C , and ^{29}Si NMR spectroscopic assignments in toluene- d_8 are given in Table 1. The ^1H and ^{13}C assignments were verified by a HETCOR experiment. Repeated elemental analyses were attempted but consistently gave poor data. This is likely a result of the sensitivity of the samples to air and also due to incomplete combustion. Anal. Found: C, 36.4; H, 9.4; N, 6.1. $\text{C}_{24}\text{H}_{72}\text{N}_4\text{Si}_8\text{MgCa}$ requires: C, 40.8; H, 10.3; N 7.9. IR: 1012 vs $[\nu_{\text{as}}(\text{Si}^{\text{N}}\text{CaSi})]$, 966 vs $[\nu_{\text{as}}(\text{Si}^{\text{N}}\text{MgSi})]$, 934 vs $[\nu_{\text{as}}(\text{Si}^{\text{N}}\text{CaMgSi})]$, 451 m $[\nu_{\text{as}}(\text{MgN}_2)]$, 416 m $[\nu_{\text{as}}(\text{CaN}_2)]$. MS (400 K, 70 eV, amu): the spectrum was identical to that of the homometallic compounds, 346 (0.5%; M^+ of $\text{Mg}(\text{HMDS})_2$ or $\text{M}^+ - \text{Me}$ of $\text{Ca}(\text{HMDS})_2$), 331 (1.3%; $\text{M}^+ - \text{Me}$ of $\text{Mg}(\text{HMDS})_2$ or $\text{M}^+ - 2 \text{ Me}$ of $\text{Ca}(\text{HMDS})_2$), 161 (3.9%; HNSi_2Me_6), 146 (100%; HNSi_2Me_5).

Synthesis of $[\text{CaN}(\text{SiMe}_3)_2\cdot(\text{pyr})_n]^+[\text{Mg}\{\text{N}(\text{SiMe}_3)_2\}_3]^-$, **4.** Dis-solution of single crystals of **3** in neat pyridine- d_5 produced solutions

(36) Shriver, D. F.; Drezdson, M. A. *Manipulation of Air-Sensitive Compounds*; John Wiley and Sons: New York, 1986.

(37) Amarego, W. L. F.; Perrin, D. D. *The Purification of Laboratory Chemicals*, 4th ed.; Butterworth Heinemann: Bath, 2002.

(38) Henderson, K. W.; Allan J. F.; Kennedy, A. R. *J. Chem. Soc., Chem. Commun.* **1997**, 1149.

containing **4**. The amount of **4** initially produced varied between experiments but was normally in the range 75–90%. Attempts to isolate **4** from solution as a pure compound have thus far been unsuccessful. ¹H NMR (400.13 MHz, pyridine-*d*₅, 25 °C): δ 0.17 (s, 18H, [Ca{N(SiCH₃)₂}]⁺), 0.62 (s, 54H, [Mg{N(SiCH₃)₂}]₃[−]). ¹³C NMR (125.704 MHz, pyridine-*d*₅, 25 °C): δ 6.30 (s, [Ca{N(SiCH₃)₂}]⁺), 7.52 (s, [Mg{N(SiCH₃)₂}]₃[−]).

Quenching Studies. A Schlenk tube under N₂ was filled with 1 mmol of base (**1**, **2**, or **3**) and 2.5 mL of pyridine. Propiophenone (0.75 mmol) was added directly into the solution at ambient temperature followed immediately by the addition of TMSCl (0.25 mL, 2 mmol). Aliquots of the solution were then removed at appropriate time periods as the reactions progressed and quenched with saturated aqueous NaHCO₃. The quenched reaction mixtures were extracted with 5 mL of ether, diluted by THF, and analyzed by GC. The stereochemical assignments for the silyl enol ethers were made by comparison with authentic samples.³⁹

Computational Details. The Gaussian 03 series of programs was used for the geometry optimization calculations for **I–III**.⁴⁰ No symmetry constraints were imposed, and the molecules were allowed to freely optimize at the B3LYP/6-31G* level using related crystal structure data as starting geometries.³⁰ The resulting geometries were then used for further optimizations at the B3LYP/6-311++G** level of theory.

X-ray Crystallography. Single-crystals of **3** were examined under Infineum V8512 oil. The datum crystal was affixed to either a thin glass fiber atop a tapered copper mounting pin or a Mitegen mounting loop and transferred to the −53 °C nitrogen stream of a Bruker APEX diffractometer equipped with an Oxford Cryosystems 700 series low-temperature apparatus. Cell parameters were determined using reflections harvested from three sets of 12 0.5° ϕ scans. The orientation matrix derived from this was transferred to COSMO⁴¹ to determine the optimum data collection strategy requiring a minimum of 4-fold redundancy. Cell parameters were refined using reflections harvested from the data collection with $I \geq 10\sigma(I)$. All data were corrected for Lorentz and polarization effects, and runs were scaled using SADABS.⁴²

(39) Heathcock, C. H.; Buse, C. T.; Kleschick, W. A.; Pirrung, M. C.; Sohn, J. E.; Lampe, J. *J. Org. Chem.* **1980**, *45*, 1066.

(40) Pople, J. A.; et al. *Gaussian 03*; Gaussian, Inc.: Wallingford CT, 2004.

(41) APEX2 and COSMO; Bruker-Nonius AXS: Madison, WI, 2005.

Table 4. Crystallographic Data for 3

empirical formula	C ₂₄ H ₇₂ CaMgN ₄ Si ₈
fw, g/mol	705.97
cryst syst	triclinic
space group	P $\bar{1}$
<i>a</i> , Å	9.1640(3)
<i>b</i> , Å	12.1080(4)
<i>c</i> , Å	21.6540(8)
α, deg	87.541(2)
β, deg	85.780(3)
γ, deg	69.550(2)
<i>V</i> , Å ³	2244.77(13)
<i>Z</i>	2
<i>T</i> , °C	−53(2)
ρ _{calc} , g/cm ³	1.044
μ(Mo Kα), mm ^{−1}	0.386
cryst size	0.25 × 0.31 × 0.32
<i>F</i> (000)	776
θ range, deg	1.89–26.35
no. of reflns collected	12 520
no. of unique reflns	8562
<i>R</i> ₁ [<i>I</i> > 2σ(<i>I</i>)] ^a	0.0544
<i>wR</i> ₂ (all data)	0.1102
GOF on <i>F</i> ²	1.055

The structure was solved and refined using SHELXTL.⁴³ Structure solution was by direct methods. Non-hydrogen atoms not present in the direct methods solution were located by successive cycles of full matrix least squares refinement on *F*². All non-hydrogen atoms were refined with parameters for anisotropic thermal motion. Hydrogen atoms were placed at idealized geometries and allowed to ride on the position of the parent atom. Hydrogen thermal parameters were set to 1.5× the equivalent isotropic *U* of the parent atom. Table 4 lists the key crystallographic parameters.

Acknowledgment. We thank Grand Valley State University and the National Science Foundation for support (CHE03-45713 and CHE-04-43233).

Supporting Information Available: Crystallographic data for **3** in CIF format. The complete list of authors for ref 40. Details of the calculations. This material is available free of charge via the Internet at <http://pubs.acs.org>.

OM060521G

(42) Sheldrick, G. M. *SADABS*; Bruker-Nonius AXS: Madison, WI, 2004.

(43) Sheldrick, G. M. *SHELXTL*; University of Göttingen.